NANO LETTERS

LETTER

pubs.acs.org/NanoLett

Aluminum for Nonlinear Plasmonics: Resonance-Driven Polarized Luminescence of Al, Ag, and Au Nanoantennas

Marta Castro-Lopez,[†] Daan Brinks,[†] Riccardo Sapienza,[†] and Niek F. van Hulst*[,†,‡]

[†]ICFO—Institut de Ciencies Fotoniques, Mediterranean Technology Park, 08860 Castelldefels (Barcelona), Spain

[‡]ICREA—Institució Catalana de Recerca i Estudis Avançats (ICREA), 08010 Barcelona, Spain

Supporting Information

ABSTRACT: Resonant optical antennas are ideal for nanoscale nonlinear optical interactions due to their inherent strong local field enhancement. Indeed second- and third-order nonlinear response of gold nanoparticles has been reported. Here we compare the on- and off-resonance properties of aluminum, silver, and gold nanoantennas, by measuring two-photon photoluminescence. Remarkably, aluminum shows 2 orders of magnitude higher luminescence efficiency than silver or gold. Moreover, in striking contrast to gold, the aluminum emission largely preserves the linear incident polarization. Finally, we show the systematic resonance control of two-photon excitation and luminescence polarization by tuning the antenna width and length independently. Our findings point to aluminum as a promising metal for nonlinear plasmonics.

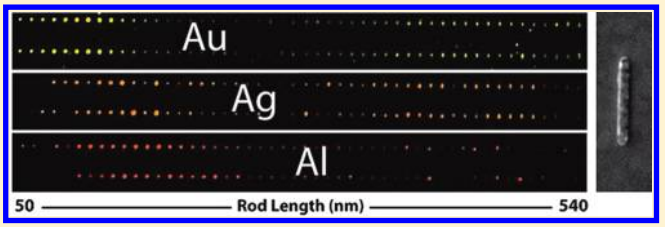

KEYWORDS: Gold, aluminum, nanoantennas, two-photon photoluminescence, nonlinear plasmonics, resonance-controlled polarization

In plasmonic systems, the incident light can be confined to subwavelength dimensions,[1] which creates intense fields, highly localized in the near-field area of metallic nanostructures.[2] The strong field confinement allows ultrasensitive detection[3] and high-resolution microscopy[4] and could enable efficient communication between single emitters.[5] More importantly, the intense localized fields provide the perfect setting for enhanced nonlinear optics at the nanoscale.[6−9] Nanoantennas of well-defined shape and dimensions are excellent building blocks to tailor the near-field[10] and to obtain controlled nonlinear signals.[11−14] These nanoantennas are currently widely explored.[15−17] Most studies are focused on gold or silver antennas, while no systematic experimental study of nonlinear signals from antennas of different metals has been performed so far. In this work we report on the nonlinear response of rod antennas of three plasmonic metals: aluminum, silver, and gold, demonstrating the performance of aluminum for nonlinear plasmonics. We study the intensity and polarization of the emission occurring upon two photon excitation.[18−20] By tuning the dimensions (width and length) of the antennas, we explore the interplay of the transversal and longitudinal resonances of the plasmon modes excited in the metal. This size-dependent interplay determines the polarization of the luminescence which is shown to be tunable and very different for each metal. In all our nonlinear measurements (TPPL and SHG measurements) aluminum is shown to be an excellent material for nonlinear optics (NLO), with a luminescence efficiency almost 2 orders of magnitude higher than the efficiency of gold and a better conservation of the incident linear polarization.

The increase in plasmon frequency from gold to silver and aluminum (2.5, 3.8, and 15 eV respectively) changes their optical response. In addition, the characteristic field distribution of the resonant antenna modes[21] is determined by the effective plasmon wavelength,[22] which is much shorter than the free-space wavelength due to the frequency dispersion of the metal. Thus, in designing the nanoantenna for a particular optical response, the intrinsic material properties play a fundamental role, together with size, shape, and physical state (crystallinity, oxidation).[23−26] Gold has been the most widely used metal in nanostructures, more stable against oxidation than silver even if the latter exhibits stronger plasmonic resonance. On the other hand, aluminum, being a relatively perfect metal with very short skin depth,[27] has been almost ignored for plasmonics applications[29,28] due to its higher losses in the visible/near-infrared spectrum compared to silver and gold.[30]

We fabricated gold, silver, and aluminum rod antennas with widths of 40 nm and lengths increasing from 50 to 540 nm, in steps of 10 nm, by electron-beam lithography (see Methods/Fabrication in the Supporting Information). Figure 1a shows the smallest and largest of the Al nanoantennas investigated. Representative two-photon photoluminescence (TPPL) confocal images (see Methods/Setup in the Supporting Information) are shown in Figure 1b where four equal rows of nanoantennas are imaged for each metal: the signal depicted is the polarization-resolved TPPL of the antennas (wavelengths from 450 to 650 nm) upon excitation with a 15 fs pulse (center wavelength 780 nm, bandwidth 120 nm)[31] and linear polarization along the long axis of the antennas. The length of the antennas increases

Received: July 3, 2011
Revised: September 22, 2011
Published: October 04, 2011

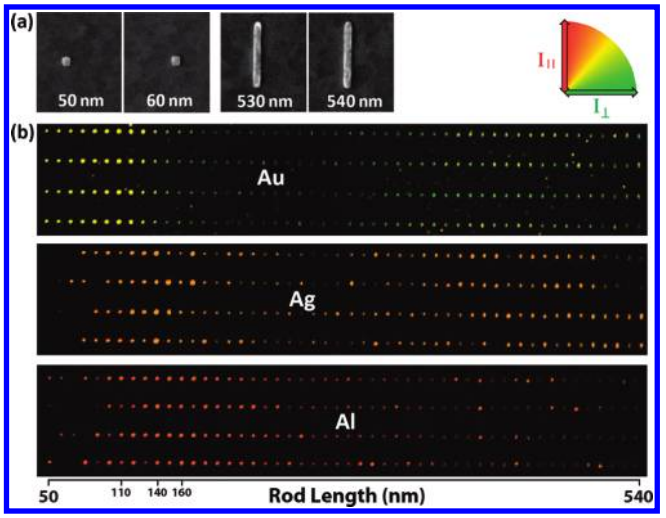

Figure 1. Luminescence of individual Au, Ag, and Al antennas of increasing length. (a) SEM image of four aluminum rods with lengths 50, 60, 530, and 540 nm. (b) TPPL image of four identical rows of gold (top), silver (middle), and aluminum (bottom) rod antennas with increasing lengths from 50 (left) to 540 nm (right) in steps of 10 nm. Bands of resonant lengths are observed for gold antennas of 110 nm, silver antennas of 140 nm, and aluminum antennas of 160 nm. The color scale represents emission polarization (inset), with red/green indicating emission polarized along and perpendicular to the antenna axi, respectively. It is clear that TPPL of aluminum is polarized parallel to the antennas while gold TPPL is nonpolarized.

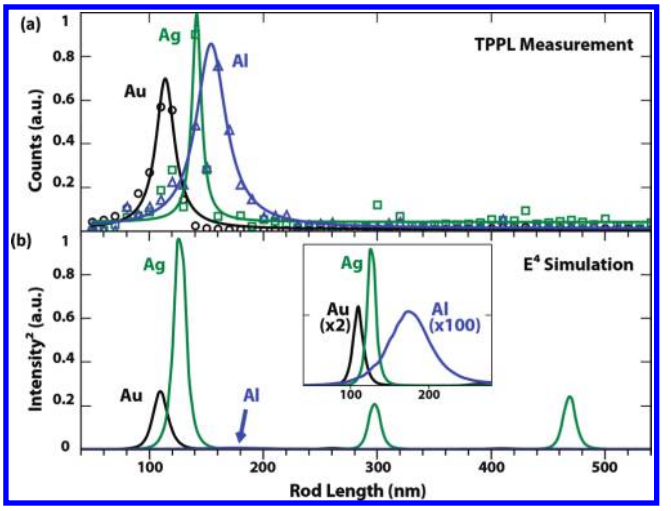

Figure 2. Antenna resonances show the plasmonic dispersion for Au, Ag, and Al. (a) Experimental resonance lengths occur at 110, 140, and 160 nm for gold, silver, and aluminum antennas, respectively, when excited with a broad band Ti:sapphire pulse (see Methods/Setup section in the Supporting Information). (b) Calculated squared intensity (I^2) as a function of antenna length. The position and width of the resonances fit well with the simulations of the integrated $|E|^4$ around the antennas; note that aluminum shows 2 orders of magnitude stronger luminescence than expected from a comparison of the $|E|^4$ (inset).

from left to right. From direct inspection of the intensity of the TPPL spots, one clearly identifies resonant rod lengths for each metal. These lengths correspond to the first dipole and third resonance modes ($L_{res} \sim \lambda_{sp}/2$ and $L_{res} \sim 3\lambda_{sp}/2$, respectively, with λ_{sp} the local surface plasmon wavelength); the second resonance corresponds to a dark mode which couples only very weakly to the incident far field. Interestingly the polarization of the luminescence, as can be seen from the color scale, is different between the three metals: aluminum shows polarization preferentially along the antenna axis, while gold shows no specific polarization direction and silver is an intermediate case.

Integrating the signal over the four rows of antennas with identical lengths shown in Figure 1, we plot in Figure 2a the TPPL intensity response as a function of the length of the antenna. We find resonances with different widths and at different resonance lengths L_{res} for the three metals: L_{res}(Au) = 110 nm, L_{res}(Ag) = 140 nm, and L_{res}(Al) = 160 nm. As expected from the low Im{ε} of silver through all the visible spectrum,[32] the resonance peak of silver antennas is the narrowest one (<20 nm FWHM in length), followed by gold (30 nm) and aluminum (50 nm). The solid lines are fittings to the data points with single peak Lorentzian curves, showing a clear resonant behavior. In Figure 2b these resonances are compared to the theoretical predictions obtained from finite difference time-domain (FDTD) simulations (see Methods/Simulation in the Supporting Information for details). The good agreement in position and width of the peaks confirms the accuracy of fabrication for the three metals. It is important to notice that in Figure 2b we plot the integral value of $|E|^4$ integrated over the volume of the antenna; in this we account for the excitation part of the TPPL process, which is modeled as being proportional to $\sim \mathrm{Im}(\chi^{(3)})|E|^4$.[33] We assume that TPPL is an incoherent process occurring after two-photon excitation. The calculations show that the actual field strength around resonant aluminum antennas is considerably lower than those around silver and gold antennas: in fact the integral $|E|^4$ for Al is calculated to be a factor of ~200 lower than that for Ag and a factor of ~50 lower than that for Au (Figure 2b inset). It is therefore striking that the Al response is so strong; in fact the measured TPPL signal is comparable for the three metals being the maximum signal of Al antennas 1.3 times higher than that of Au antennas. If, from Figure 2, we deduce the luminescence efficiency as the ratio between measured TPPL intensity and simulated excitation intensity squared, we obtain for aluminum around 2 orders of magnitude higher luminescence efficiency than for gold or silver (factors of ~70 and ~160, respectively). This can be partially attributed to a larger $\mathrm{Im}(\chi^{(3)})$ (larger two-photon absorption) and partially to a different intrinsic emission efficiency (η) of the material.

The performance of aluminum in TPPL, an incoherent third-order nonlinear process, goes along with our observation of strong second-harmonic generation (SHG) of aluminum, which instead is a coherent second-order nonlinear process[34] (see Methods/Second and Third Order Susceptibilities in the Supporting Information). The literature $\chi^{(2)}$ values for aluminum thin films are 1 order of magnitude higher than those for the other two metals.[35] However, it is not trivial to extrapolate these results to nanoparticles,[36−39] where $\chi^{(2)}$ and $\chi^{(3)}$ are mainly dominated by symmetry breaking surface effects, which are related to the metal grain size, crystallinity, and specific details of the sample growth. These are critical aspects, especially in the case of aluminum since the interband transition does not occur between d-shell and conduction band, as in gold and silver, but instead between occupied and unoccupied conduction bands. Allowed transition between these bands depends strongly on the degree of crystallinity.[26] It is therefore very challenging to predict the nonlinear response on the nanoparticle level, and experimental

dx.doi.org/10.1021/nl202255g |*Nano Lett.* 2011, 11, 4674–4678

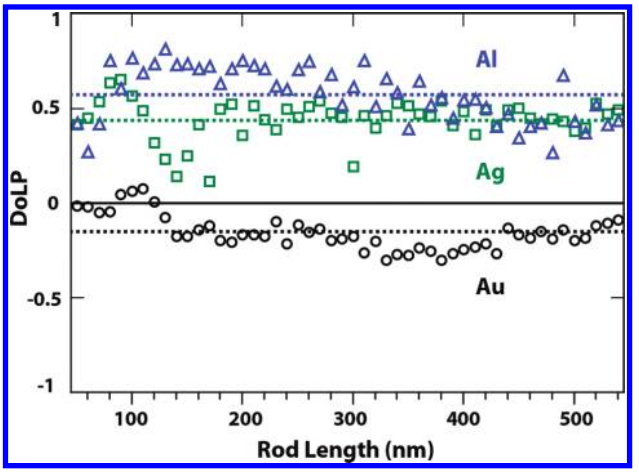

Figure 3. Degree of linear polarization of gold, silver, and aluminum antennas as a function of length. While the TPPL of aluminum antennas is highly polarized, TPPL of silver is partially polarized and the TPPL from gold is largely unpolarized.

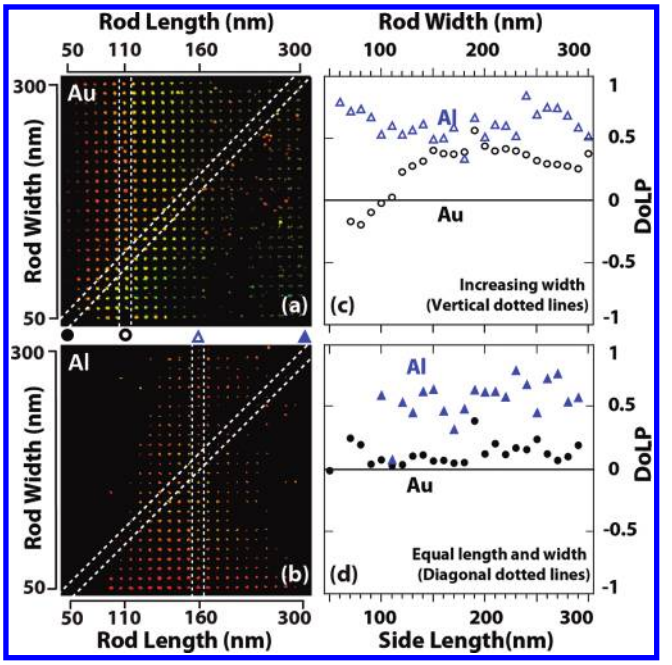

Figure 4. Comparison of the polarization of TPPL from gold and aluminum patches. Polarization resolved images of TPPL from matrices of gold (a) and aluminum (b) patches with lengths varying from 50 to 300 nm (horizontal axis) and widths varying from 50 to 300 nm (vertical axis). (c) Comparison of the DoLP from aluminum and gold patches as a function of rod width at the excitation resonance condition marked by the vertical dotted lines of L_{res}(Au) = 110 nm and L_{res}(Al) = 160 nm. A resonant behavior in the polarization of the TPPL is clear. (d) Comparison of the DoLP from aluminum and gold nanosquares (marked by the diagonal dotted lines) as a function of side length. The higher intrinsic polarizability of aluminum is visible.

measurements of the nonlinear strength are valuable. The high intensity of the generated TPPL and SHG make aluminum nanoantennas suitable components for the localized generation of both second- and third-order nonlinear signals from Ti:sapphire pulses.

Interestingly, the polarization of the luminescence upon nonlinear excitation is different for the three metals. This difference is shown in the color scale in Figure 1b (inset) and can be quantified by the degree of linear polarization (DoLP), defined as $(I_{\parallel} - I_{\perp})/(I_{\parallel} + I_{\perp})$. Here $I_{\parallel}$ is the component of the luminescence with polarization along the long axis of the antenna and thus with the same polarization as the incident light and $I_{\perp}$ is the perpendicular component.

In Figure 3 we plot the DoLP of the TPPL from antennas of the different metals as a function of antenna length. The emission from aluminum follows almost uniformly the incident polarization with values of DoLP up to 0.8. The TPPL from silver is also largely polarized along the excitation/antenna direction and it shows a resonance type dip around the length range of maximum emission. In contrast, TPPL from gold antennas tends to be uniformly unpolarized or even slightly polarized perpendicular to the antenna axis. The average values and standard deviations over all antenna lengths are DoLP(Au) = -0.15 ± 0.09, DoLP(Ag) = 0.44 ± 0.11, and DoLP(Al) = 0.57 ± 0.14, where DoLP = 0 corresponds to equal signal in both polarization directions (solid line).

If the absorption and emission processes leading to TPPL generation were mediated by a dipolar interaction between the metal in the antenna and the excitation field, we would have expected that, on average, the polarizibility of the antennas would have followed the polarization of the excitation field, regardless of the metal. In our 1.3 NA objective this would lead to a slight mixing of field components (Ez^2/Ex^2 = 0.097 and Ey^2/Ex^2 = 0.0695) for incoming x-polarization[40] (Ez being the out of plane component), which would lead to a decrease of the DoLP from 1 to 0.86. Nevertheless it could not explain the extreme depolarization values observed for gold where the transversal component of the polarization is slightly stronger than the longitudinal one. We attribute the observed depolarization response to the presence of both longitudinal and transversal modes in the structure.[41] By tuning the nanoantenna resonance to the TPPL emission wavelength, one modifies the polarization of the emission for specific antenna dimensions. For a proof of concept we chose the two metals presenting extreme polarization differences: aluminum (highly polarized) and gold (completely unpolarized). In order to disentangle the contribution of the transverse and longitudinal resonance, and of the excitation and emission resonance, the polarization of TPPL was investigated as a function of both antenna length and width independently. The polarization of the excitation was kept linear and oriented along the rod length as defined in Figure 4.

TPPL response on an array of gold and aluminum antennas is shown in panels a and b of Figure 4, respectively. By controlling both the width (vertical axis) and the length (horizontal axis) of the nanorods (see Methods/Fabrication in the Supporting Information), the resonance structure can be fully mapped in both directions independently. The plasmonic resonance of the excitation band (λ_{exc} = 780 nm) with the previously determined rod lengths of L_{res}(Au) = 110 nm and L_{res}(Al) = 160 nm (shown in panels a and b of Figure 4 with the vertical dotted lines) can clearly be recognized in the intensity of the measured signal. This resonance condition moves slightly to longer rods while the width is increasing as expected for rods with a larger cross section.[42] At first inspection of Figure 4a, the polarization of the TPPL of gold nanorods changes from perpendicular (color-coded green) to mixed polarization (color-coded yellow) and to parallel (color-coded red) when increasing the rod width. Instead, in the case of

dx.doi.org/10.1021/nl202255g |Nano Lett. 2011, 11, 4674–4678

aluminum (Figure 4b) the polarization changes from parallel (color-coded red) to mixed polarizations (color-coded yellow) to parallel again. A quantitative analysis of this polarization response of the resonant nanorods (vertical dotted lines) is plotted in Figure 4c. The polarization of the TPPL of both Au and Al antennas has a clear resonant evolution with increasing width. The peak of this resonant evolution occurs for rods of widths $W(\mathrm{Au}) = 70$ nm and $W(\mathrm{Al}) = 140$ nm which matches exactly the length for the emission resonances for the TPPL wavelengths with peak at 600 nm (see Methods/Simulations in the Supporting Information). When the nanorod width is resonant with the emission, aluminum shows a downward deviation of DoLP from the otherwise highly polarized TPPL, while gold shows a larger variation, from completely unpolarized DoLP = −0.19 at the emission resonance, to slightly polarized DoLP = 0.56 to less polarized DoLP = 0.25. Therefore the data show that polarization of the TPPL is given by the competition between the plasmon resonances polarized in the rod length and in the rod width direction.

The polarization of third-order nonlinear emission from metallic antennas can be tuned by shifting the emission bands in and out of resonance with the width of the antennas. The range of tunability seems to be related to the material intrinsically. To check the inherent polarizability of each metal, we compare the polarization of the TPPL coming from nanosquares (length equal to width) of different size (Figure 4, diagonal dotted lines). Any geometrical resonance of the emission band should effectively be canceled out due to the square symmetry. However, we measured consistently a different polarization response between gold and aluminum: $\mathrm{DoLP(Au)} = 0.13 \pm 0.09$ and $\mathrm{DoLP(Al)} = 0.56 \pm 0.16$ as shown in Figure 4d. There is an inherent limit for the tunability of the polarization of aluminum luminescence related to the higher polarizability of this material. The reason for this intrinsic difference between gold and aluminum is still subject of investigation; it is probably related to the degree of crystallinity given by the different grain size[43] (∼20 nm for gold and ∼80 nm for aluminum), the different nature and location of the interband transitions (d-band electrons for gold and conduction electrons for aluminum; at 500 and 800 nm respectively),[26] and the different number of free-electrons in the conduction band. Polarized emission has been reported in the case of crystalline gold rods;[44] however, further studies on the matter would be needed in order to develop a model which could explain these intrinsic polarizability differences.

In conclusion, we presented a detailed experimental study of the nonlinear response of optical rod antennas. Two-photon photoluminescence from gold, silver, and aluminum antennas was investigated. Aluminum shows around 2 orders of magnitude stronger nonlinear response than gold or silver. We have shown how nanoantennas generate localized nonlinear signals and the flexibility they provide in adapting the polarization of the generated emission by changing the antenna dimensions. This has important applications in plasmonic parametric conversion and highly localized coherent control in complex environments. Finally, we propose aluminum as a suitable material for plasmonic antennas; due to its high luminescence efficiency, inherent large polarizability, and better radiator in the near-UV/visible wavelength range, it is particularly appropriate for nonlinear plasmonics.

■ ASSOCIATED CONTENT

Supporting Information. Detailed fabrication, setup, and simulation information with corresponding figures and spectra of Au and Al nanoantennas and discussion of second- and third-order susceptibilities. This material is available free of charge via the Internet at http://pubs.acs.org/.

■ AUTHOR INFORMATION

Corresponding Author
*E-mail: Niek.vanHulst@ICFO.es.

■ ACKNOWLEDGMENT

We wish to thank L. Novotny and T. H. Taminiau for fruitful discussions. This research was funded by the MICINN, programs FIS2009-08203, CONSOLIDER CSD2007-046, RyC, Fundació CELLEX, and the EU ERC Grant No. 247330.

■ REFERENCES

(1) Barnes, W. L.; Dereux, A.; Ebbesen, T. W. *Nature* **2003**, *424*, 14.
(2) Markel, V. A.; Shalaev, V. M.; Zhang, P.; Huynh, W.; Tay, L.; Haslett, T. L.; Moskovits, M. *Phys. Rev. B* **1999**, *59*, 10903.
(3) Willets, K. A; Van Duyne, R. P. *Annu. Rev. Phys. Chem.* **2007**, 58.
(4) Hoeppener, C.; Novotny, L. *Nano Lett.* **2008**, *8*, 642–646.
(5) Martin-Cano, D.; Martin-Moreno, L.; Garcia-Vidal, F. J.; Moreno, E. *Nano Lett.* **2010**, *10*, 3129–3134.
(6) Boyd, R. W. *Nonlinear Optics*; Academic Press: Boston, MA, 1992.
(7) Hache, F.; Ricard, D.; Flytzanis, C. *J. Opt. Soc. Am. B* **1986**, *3* (12), 1647–1655.
(8) Renger, J.; Quidant, R.; van Hulst, N. F.; Palomba, S.; Novotny, L. *Phys. Rev. Lett.* **2009**, *103*, 266802.
(9) Schumacher, T.; Kratzer, K.; Molnar, D.; Hentschel, M.; Giessen, H.; Lippitz., M. *Nat. Commun.* **2011**, *2*, 333.
(10) Mühlschlegel, P.; Eisler, H. J.; Martin, O. J. F.; Hecht, B.; Pohl, D. W. *Science* **2005**, *308*, 1607–1609.
(11) Ghenuche, P.; Cherukulappurath, S.; Taminiau, T. H.; van Hulst, N. F.; Quidant, R. *Phys. Rev. Lett.* **2008**, *101*, 116805.
(12) Biagioni, P.; et al. *Phys. Rev. B* **2009**, *80*, 045411.
(13) Ko, K. D.; et al. *Nano Lett.* **2011**, *11*, 61–65.
(14) Hanke, T.; Krauss, G.; Träutlein, D.; Wild, B.; Bratschitsch, R.; Leitenstorfer, A. *Phys. Rev. Lett.* **2009**, *103*, 257404.
(15) Curto, A. G.; Volpe, G.; Taminiau, T. H.; Kreuzer, M.; Quidant, R.; van Hulst, N. F. *Science* **2010**, *329*, 930–933.
(16) Farahani, J. N.; Pohl, D. W.; Eisler, H. J.; Hecht, B. *Phys. Rev. Lett.* **2005**, *95*, 017402.
(17) van Nieuwstadt, J. A. H.; et al. *Phys. Rev. Lett.* **2006**, *97*, 146102.
(18) Boyd, G. T.; Yu, Z. H.; Shen, Y. R. *Phys. Rev. B* **1986**, *33*, 7923.
(19) Denk, W.; Strickler, J. H.; Webb, W. W. *Science* **1990**, *248*, 73–76.
(20) Berversluis, M. R.; Bouhelier, A.; Novotny, L. *Phys. Rev. B* **2003**, *68*, 115433.
(21) Taminiau, T. H.; Moerland, R. J.; Segerink, F. B.; Kuipers, L.; van Hulst, N. F. *Nano Lett.* **2007**, *7*, 28–33.
(22) Novotny, L. *Phys. Rev. Lett.* **2007**, *98*, 266802.
(23) Pelton, M.; Aizpurua, J.; Bryant, G. *Laser Photonics Rev.* **2008**, *2*, 136–159.
(24) Bryant, G. W.; Garcia de Abajo, F. J.; Aizpurua, J. *Nano Lett.* **2008**, *8* (2), 631–636.
(25) Ekinci, Y.; Solak, H. H.; Löffler, J. F. *J. Appl. Phys.* **2008**, *104*, 083107.
(26) Palik, E. D. *Handbook of Optical Constants of Solids*; Academic Press: Orlando, FL, 1985; Vol. I.
(27) Dyson, F. J. *Phys. Rev.* **1955**, *98*, 349–359.
(28) Chan, G. H.; Zhao, J.; Schatz, G. C.; Van Duyne, R. P. *J. Phys. Chem. C* **2008**, *112* (36), 13958–13963.
(29) Taminiau, T. H.; Stefani, F. D.; Segerink, F. B.; van Hulst, N. F. *Nat. Photonics* **2008**, *2*, 234–237.
(30) Garcia de Abajo, F. J. *Rev. Mod. Phys.* **2007**, *79*, 4.

(31) Hildner, R.; Brinks, D.; Stefani, F. D.; van Hulst, N. F. *Chem. Phys. Phys. Chem.* **2010**, *10*, 1039.
(32) Bohren, C. F.; Huffman, D. R. *Absorption and Scattering of light by small particles*; Wiley: New York, 1983.
(33) Bhawalkar, J. D.; He, G. S.; Prasad, P. N. *Rep. Prog. Phys.* **1996**, *59*, 1041.
(34) Butet, J.; et al. *Nano Lett.* **2010**, *10*, 1717–1721.
(35) Krause, D.; Teplin, C. W.; Rogers, C. T. *J. Appl. Phys.* **2004**, *96*, 7.
(36) Dadap, J. I.; Shan, J.; Eisenthal, K. B.; Heinz, T. F. *Phys. Rev. Lett.* **1999**, *83*, 4045–4048.
(37) Neacsu, C. C.; Reider, G. A.; Raschke, M. B. *Phys. Rev. B* **2005**, *71*, 201402.
(38) Finazzi, M.; Biagioni, P.; Celebrano, M.; Duò, L. *Phys. Rev. B* **2007**, *76*, 125414.
(39) Zdanowicz, M.; Kujala, S.; Husu, H.; Kauranen, M. *New J. Phys.* **2011**, *13*, 023025.
(40) Novotny, L.; Hecht, B. *Principles of Nano-Optics* Cambridge University Press: Cambridge and New York, 2006.
(41) Wissert, M. D.; Moosmann, C.; Ilin, K. S.; Siegel, M.; Lemmer, U.; Eisler, H.-J. *Opt. Express* **2011**, *19*, 3686–3693.
(42) Taminiau, T. H.; Stefani, F. D.; van Hulst, N. F. *Nano Lett.* **2011**, *11*, 1020–1024.
(43) Boyd, G. T.; Yu, Z. H.; Shen, Y. R. *Phys. Rev. B* **1986**, *33*, 12.
(44) Imura, K.; Nagahara, T.; Okamoto, H. *J. Phys. Chem. B* **2005**, *109*, 13214–13220.